Direct Determination of the Base-Pair Force Constant of DNA from the Acoustic Phonon Dispersion of the Double Helix

L. van Eijck,[1,2,*] F. Merzel,[3] S. Rols,[2] J. Ollivier,[2] V. T. Forsyth,[2,4] and M. R. Johnson[2]

[1]*Reactor Institute Delft, Delft University of Technology, Mekelweg 15, 2629JB, Delft, The Netherlands*
[2]*Institut Laue-Langevin, 6 rue Jules Horowitz, BP156 38042, Grenoble, France*
[3]*National Institute of Chemistry, Hajdrihova 19, 1000 Ljubljana, Slovenia*
[4]*EPSAM/ISTM, Keele University, Staffordshire, ST5 5BG, United Kingdom*

(Received 19 October 2010; published 19 August 2011)

Quantifying the molecular elasticity of DNA is fundamental to our understanding of its biological functions. Recently different groups, through experiments on tailored DNA samples and numerical models, have reported a range of stretching force constants (0.3 to 3 N/m). However, the most direct, microscopic measurement of DNA stiffness is obtained from the dispersion of its vibrations. A new neutron scattering spectrometer and aligned, wet spun samples have enabled such measurements, which provide the first data of collective excitations of DNA and yield a force constant of 83 N/m. Structural and dynamic order persists unchanged to within 15 K of the melting point of the sample, precluding the formation of bubbles. These findings are supported by large scale phonon and molecular dynamics calculations, which reconcile hard and soft force constants.

DOI: 10.1103/PhysRevLett.107.088102 PACS numbers: 87.14.gk, 63.22.−m, 78.70.Nx, 87.10.Tf

DNA stores the genetic code of all living organisms. Its principle biological functions of DNA are therefore transcription and replication. These processes take place in cells where DNA undergoes protein-mediated, mechanical manipulation resulting in folding, coiling and denaturing of the DNA molecule. The elasticity of DNA also underpins cleavage by enzymes [1] and the formation of 'bubbles' of locally denatured zones along the helix [2,3]. Models describing biologically relevant processes depend on the mechanical properties of DNA expressed as parameters, such as the base-pair force constant, which is crucial in the process of denaturing of DNA [4,5]. All measurements of DNA elasticity are therefore important in understanding the biological function of DNA and here we focus on stretching elasticity and the underlying base-pair stacking interaction.

Recently considerable progress has been made in measuring the flexibility of the DNA helix although one concern is the extent to which the experimental or theoretical approaches themselves influence the results [6]. From well-defined oligomers of DNA, the stretch-torsion coupling can be obtained via magnetic tweezers and measuring the consequent over- or under-winding of the helix by tracking an attached rotor bead. In the work of Gore *et al.* [7], a stretching elastic modulus is reported, which equates to an inter base-pair force constant of 3 N/m. Another example of a molecular sculpturing approach involves DNA oligomers capped with gold nanoparticles, which allow the end-to-end distance to be measured by small angle x-ray scattering [8]. This work reported corresponding values 10 times smaller: 0.3 N/m. Similarly, Wiggins *et al.* [9] extracted bending force constants from single DNA molecule conformations on a substrate. They too found that the corresponding force constants are much smaller on a local length scale than predicted by classical elasticity models. A more theoretical approach [10] uses the well-known melting temperatures of DNA to calculate the flexibility on a local length scale via the Peyrard-Bishop model [11], assuming that all thermodynamic energy is stored in the vibrational dynamics. The resulting stretching force constant is estimated to be 0.4 N/m. Brillouin scattering experiments have reported a range of sound velocities [12] which can be equated to a stretching force constant ranging from 67 to 133 N/m. Despite the importance of these results, reported values vary by 3 orders of magnitude and yet there has been no attempt to reconcile these results. An initial observation is that structure and solution-based measurements and analysis give low force constants.

The most direct approach to obtain force constants is via vibrational dynamics and, in particular, the longitudinal acoustic phonons along the helix when the base-pair stacking interaction is of interest. Early work includes the inelastic neutron scattering (INS) experiments of Grimm *et al.* [13,14] which was later extended by Krisch *et al.* [15] and Liu *et al.* [16] using inelastic X-ray scattering (IXS). Dispersion relations obtained from the two sets of IXS experiments are similar despite the samples being in different forms, wet-spun films [15] and pastes oriented between glass slides [16], and having different aqueous concentrations and cation valencies. On the other hand, INS and IXS experiments were performed on similar wet-spun films [17] and yet the measured dispersion relations result in sound velocities differing by almost a factor of 2 (1.85 km/s from INS and 3.0 km/s from IXS).

The phonon dispersion measured by IXS in the direction of the helical axis was later reproduced by atomic scale,

force field based, phonon calculations [18]. The periodic model, based on a random, 10 base-pair sequence, counterions and water to fill the simulation box, accommodates short-range disorder corresponding to the reported, liquid-like description of DNA [15,16]. However, the phonon calculations also revealed acoustic modes that are much softer than those reported by IXS and have a wave-vector dependence characteristic of the longer length scale corresponding to the helix pitch.

In this context, we report unique measurements of longitudinal acoustic and optic phonons using a new INS spectrometer to investigate the discrepancy between dispersion relations obtained from INS and IXS experiments and to test the computer prediction of still softer longitudinal acoustic phonons. The measurements have been performed over a wide temperature range, from 70 K almost up to melting (335 K), to investigate structural integrity and the possibility of bubble formation. They give direct access to the base-pair stacking interaction. Atomistic simulations are used to gain insight into the widely varying force constants resulting from scattering measurements and other techniques, reported above.

The measurements were performed on wet-spun, oriented fibres of Li-DNA in the B form, which were prepared as described by Rupprecht [17]. Relative humidity is one factor determining the structural form of DNA. It was set to 75% during the deuteration of the water and labile, DNA protons using a saturated solution of NaCl in D_2O in a desiccator containing the sample. Partially deuterated samples obtained this way minimize the incoherent scattering from the sample and therefore highlight the coherent scattering from the acoustic and optic phonons. These samples contain more than 40 water molecules per base-pair, the interhelix separation being $\sim$24 Å. The sample was sealed in a flat aluminum holder, effectively fixing the humidity level, as in other, recent neutron scattering experiments [19]. The sample has been used for diffraction studies and presents a well-defined B-DNA structure, as reported by Langridge *et al.* [20] Arnott *et al.* [21] and more recently Fuller *et al.* [22]. In this concentrated form of DNA, fibres are aligned to within a few degrees which is a requirement of the scattering experiment. The film can therefore be regarded as a constraint in the same way that the solution-based measurements, reported above, require molecular sculpturing. However, the IXS experiments performed on significantly different samples indicate that the phonons polarized along the helix axis are not very sensitive to the form of the sample, a point developed below with simulations.

INS measurements were performed on the cold neutron, time-of-flight spectrometer IN5 at the ILL. This instrument has been completely renewed in recent years, including the installation of a 30 m^2, position sensitive detector, which offers a wave-vector resolution of about 0.005 $Å^{-1}$. Exploiting this resolution requires a high neutron flux which other spectrometer developments have ensured. Compared to IXS, cold neutron spectroscopy offers an order of magnitude better energy resolution ($\sim$ 0.1 meV FWHM) and a triangular (rather than Lorentzian) shaped resolution function, which are prerequisites for these measurements.

Longitudinal, acoustic phonons are measured by orienting the DNA fibres in the neutron beam, such that the momentum transfer vector $\mathbf{Q}$ of the scattered neutrons is aligned with the characteristic, B form, Bragg peak vector τ of the DNA base pairs (rise = 3.4 Å for B DNA). By varying the wavelength of the incoming neutron beam, we focus on either the inelastic region of $S(Q, \omega)$ on the anti-Stokes side of the Bragg peak (configuration 1), or the elastic region around the Bragg peak (configuration 2). Whereas IXS measurements have been performed across a wide range of momentum transfer, these INS measurements can only be performed in the vicinity of the Bragg peak where the elastic and inelastic scattering is most intense.

In Fig. 1 the neutron scattering spectra are shown for *configurations 1 and 2*. Away from the elastic line in *configuration 1* [Fig. 1(a)] the acoustic branch seems to merge with a low-lying optical branch, but their separation is better seen in the constant-Q cuts [Fig. 1(b)]. Optic modes in this energy range have been reported previously [23] but they were assigned as interhelix modes, which is not consistent with our data or the atomistic model discussed above [18]. It is clear from these data that a low frequency, acoustic mode exists, as predicted by Merzel *et al*, that can only be measured with the high resolution in both momentum and energy transfer. The dispersion branch has its maximum at approximately 1.7 meV, nearly an order of magnitude lower than the previously reported branch ($\sim$ 12 meV) [15]. To extract the energy dispersion of the acoustic phonon, the data were fitted with a damped harmonic oscillator model, including a sinusoidal dependence of the acoustic mode frequency on wave vector. The result of these fits is shown in [24] and the corresponding dispersion relation is compared to previously reported data [18] in Fig. 2.

The data in Figs. 1(a)–1(d) were measured at 70 K. The existence of the base-pair Bragg peak well above physiological temperatures ($T > 310$ K) [19] means that structural integrity is maintained and that the acoustic mode may persist at these temperatures. By increasing temperature, quasielastic neutron scattering (QENS), mainly from water, tends to dominate the inelastic scattering. An approximate correction can be made by assuming that the QENS is isotropic and can therefore be measured by orienting the sample with the DNA fibres perpendicular to the scattering plane of the instrument. This spectrum is then subtracted from the spectrum with fibers in configuration 2. Figure 3(b) shows the difference spectra at 335 K, $\sim$15 K below the melting temperature of this DNA sample. The phonon branch can still be resolved confirming

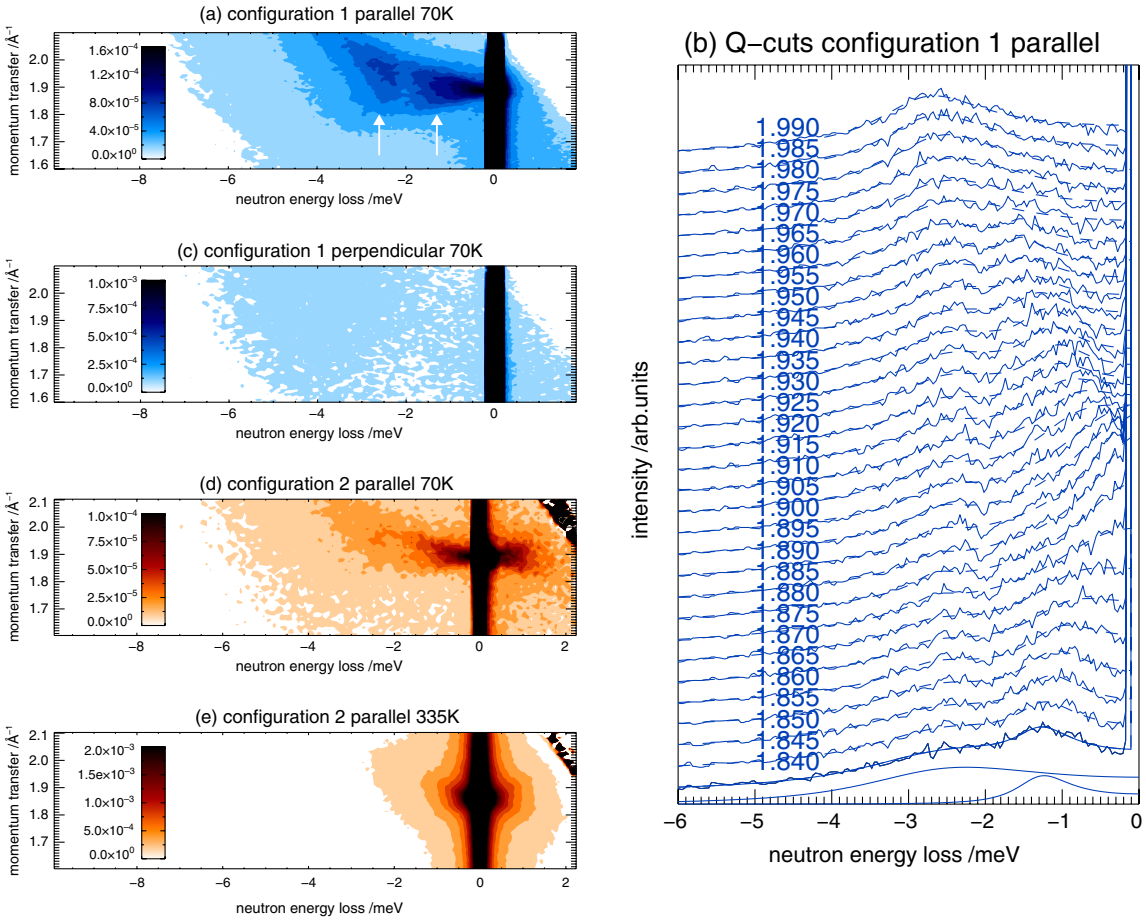

FIG. 1 (color online). The scattering intensity $S(Q, E)$ of the aligned DNA samples as measured at 70 K on the cold neutron, chopper spectrometer, IN5 at the ILL, France. In *configuration 1* the steep dispersion of the acoustic phonon is visible on the anti-Stokes side of the base pair Bragg peak [right arrow in (a)] together with the optic mode (left arrow). The constant-Q cuts of (a) are plotted in (b). The dispersion of the optic mode is extract from the fits. When DNA fibres are rotated from the parallel to perpendicular with respect to the instrumental scattering plane none of these features is visible (c). In *configuration 2* the acoustic phonon scattering is observed on both sides of the elastic line (d)

that the helical structure persists at 335 K on a longer length scale than that indicated by the Bragg peak itself.

The dispersion relations obtained from two kinds of inelastic scattering data, INS (this work) and IXS [15,16], can now be reconciled in terms of two Brillouin zones: the base-pair Brillouin zone defined by the base-pair rise of 3.4 Å and a Q-range of 1.9 $Å^{-1}$ and the helix Brillouin zone defined by the helix pitch of 34 Å, with a corresponding Q-range of 0.19 $Å^{-1}$. While Merzel *et al.* [18] have shown that the phonon branches measured by IXS are the result of many optic modes of the helix with polarization in the direction of the DNA fibre axis, the IXS data, with an approximately sinusoidal rise and fall of the inelastic intensity from 0 to 1.88 $Å^{-1}$, can be interpreted in terms of a one-dimensional, monoparticle (base-pair) chain, with a periodicity of the base-pair rise (3.4 Å). The maximum frequency (12 meV) at the Brillouin zone boundary (0.94 $Å^{-1}$) gives the average inter base-pair force constant of 83 N/m (calculated from $k_{\mathrm{avg}} = \omega_{\mathrm{max}}^2 M_{\mathrm{avg}}/4$ where M_{avg} is the average mass of a pair of nucleotides). This value is consistent with the sound velocity of 3.0 km/s reported from IXS measurements [15]. The sound velocity obtained from the new INS data in FIG. 2, 4.3 km/s, is still higher due to the better energy and wave-vector resolution.

In Fig. 4 the coherent scattering function $S(Q, E)$ is plotted for Q aligned along the helix axis, as obtained by Merzel *et al.* [18] from an atomistic phonon calculation based on an optimized, equilibrium structure. A broad band of intensity forms a pseudo acoustic phonon branch, which compares well with the experimentally obtained "base-pair phonon branch" [15]. Figure 4 also shows the low-lying acoustic phonon that reaches its maximum below 2 meV. This calculation on a random sequence of base-pairs (see [18] for details) has been repeated for a pure adenine-thymine (A-T) sequence. A similar map of the scattering function is obtained indicating that the dispersion reported here is a signature of the helix structure

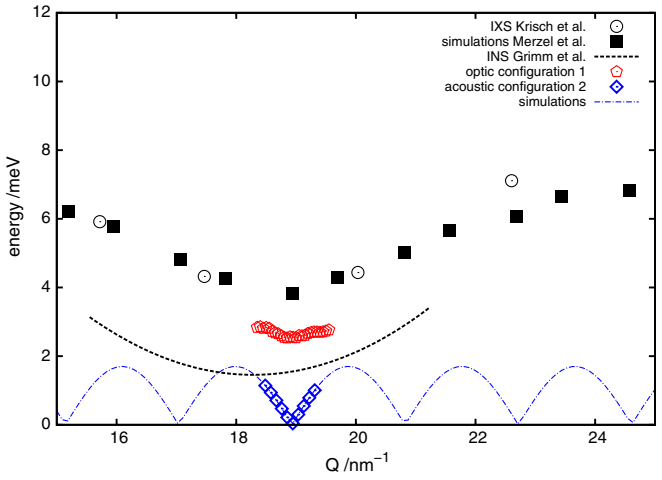

FIG. 2 (color online). Comparison of the dispersion curves of IXS (open circles) [15], calculations (filled squares) [18] and INS (dashed parabola) [13] with our fitted dispersion curves obtained in *configuration 1* (red pentagons) and 2 (blue diamonds). The dispersion curve as previously reported from INS data is probably a convolution of the optic and acoustic modes measured in this work. The sound speed obtained from the acoustic dispersion curve at the base-pair Bragg peak is 4.3 km/s.

and is not a consequence of the variability of the interaction between different base pairs. The sound velocity of the pure A-T model is 10% higher than that of the mixed sequence model, corresponding to a 20% higher, average elastic constant. In addition, phonon calculations have been performed on a set of models with different water content and on models which reproduce the lateral DNA packing according to the known crystallographic structures, including A-form DNA. In this set of models the interhelix spacing varies from 22 Å to 30 Å, demonstrating that the results reported here for modes polarised along the helix do not depend significantly on this parameter and therefore the DNA/water ratio.

The inter base-pair force constant obtained in the foregoing analysis is two to 3 orders of magnitude higher than those obtained from recent, mainly solution studies. While it is tempting to attribute this difference to the concentrated form of our samples, the phonon calculations, which mimic the fibre samples over a range of concentrations, indicate that this is not the case. An alternative computational approach is to determine the average potential energy of structures that are longer or shorter along the helix axis than the equilibrium structure used in the phonon calculation. Molecular dynamics simulations were therefore performed with the CHARMM force field, as used in the phonon calculations. For each stretched (or shortened) DNA model (12 in total), equilibrium MD simulations were performed in the *NPT* ensemble with the cell parameter along the helix constrained, followed by 1 ns production runs in the *NVE* ensemble. The average potential energy was extracted from the production runs and plotted against the corresponding helix pitch of the models. The complete set of calculations was performed at 100 K. An approximately harmonic variation of the energy as a function of helix pitch gives an effective force constant of 2.5 N/m. This value is much lower than the one extracted from phonon dispersion relations and is closer to the values obtained, for example, from structure based, solution measurements. Computationally, the same structural model

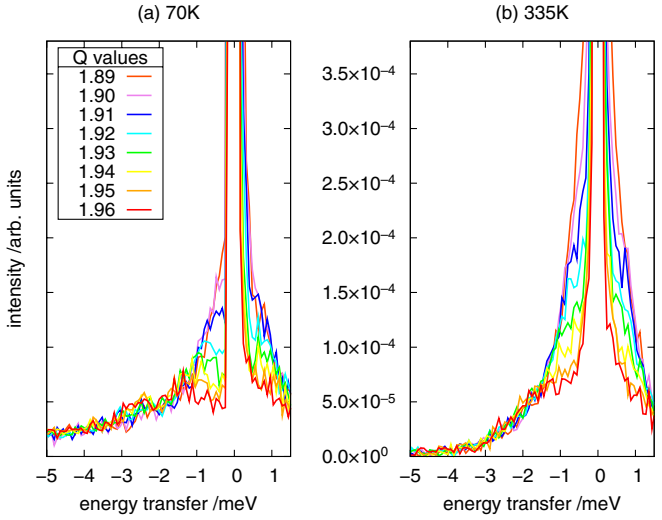

FIG. 3 (color online). Constant-Q cuts of $S(Q, E)$ of *configuration 2* at 70 K (a) and 335 K (b). In (b) the quasielastic intensity is subtracted as described in the text. The intensity of the 335 K data are rescaled by the Bose factor for comparison with the 70 K data.

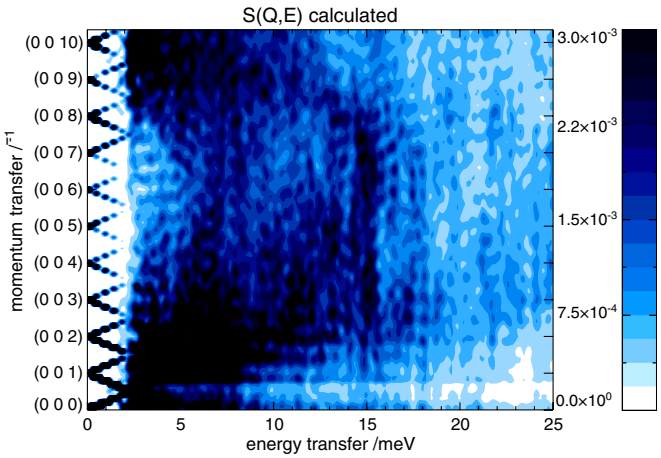

FIG. 4 (color online). A contour map of the calculated scattering intensity (logarithmic scale) versus energy transfer and Q (labeled in terms of the Brillouin zones of the helix) from phonon calculations [18]. The new INS data corresponds to the acoustic mode centered at (0,0,10) and the lower limit of the optic modes intensity at about 2 meV. The published IXS data [15] corresponds to the sinusoidal arc of intensity extending from (0,0,0) to (0,0,10), with a broad maximum at ~10 meV and $Q = (0, 0, 5)$.

and simulation engine give a high force constant from the phonon calculation, which corresponds to an instantaneous perturbation of an equilibrium structure, and a low force constant from the MD simulations due to structural reorganization of the DNA, solvent and counter ions, as occurs in solution.

The unique, experimental result presented here is the first observation of the longitudinal acoustic phonon along the helix axis, which is the only collective excitation that unequivocally reflects the helical structure of DNA via the Q dependence of the dispersion. Moreover, in contrast to the base-pair Bragg peak, which mainly probes short-range order [19], this acoustic phonon probes the structural integrity of DNA on the length scale of the helical pitch and beyond. Data measured up to 335 K show that long range, helical order persists almost up to melting and is not significantly perturbed by the formation of bubbles.

The new INS data allow a clear interpretation of the IXS data in terms of a monoparticle chain giving an inter base-pair force constant of 83 N/m. Simulations show that structural reorganization which occurs in structure- and solution-based measurements, results in much lower force constants. This work therefore gives a coherent understanding of a wide body of work on the elasticity of DNA, it underpins ongoing work on the overstretching of DNA [25,26], which shows that DNA unwinds and unzips because the force constant for stretching double-strand DNA is so high, and it provides an experimentally determined, fundamental value for understanding the stretching elasticity of DNA and therefore its biological function.

We are grateful to J. Valle-Orero, A. Wildes, M. Peyrard and N. Theodorakopoulos for fruitful discussions. We thank H. Grimm and A. Rupprecht for the wet spinning apparatus.

*l.vaneijck@tudelft.nl

[1] B. Heddi, J. Abi-Ghanem, M. Lavigne, and B. Hartmann, J. Mol. Biol. **395**, 123 (2010).
[2] M. Peyrard, Nature Phys. **2**, 13 (2006).
[3] T. S. van Erp, S. Cuesta-Lopez, J. G. Hagmann, and M. Peyrard, Phys. Rev. Lett. **95**, 218104 (2005).
[4] T. Dauxois, M. Peyrard, and A. R. Bishop, Phys. Rev. E **47**, R44 (1993).
[5] J. Kim, J. Jeon, and W. Sung, J. Chem. Phys. **128**, 055101 (2008).
[6] R. Lavery, A. Lebrun, J. Allemand, D. Bensimon, and V. Croquette, J. Phys. Condens. Matter **14**, R383 (2002).
[7] J. Gore *et al.*, Nature (London) **442**, 836 (2006).
[8] R. S. Mathew-Fenn, R. Das, and P. A. B. Harbury, Science **322**, 446 (2008).
[9] P. A. Wiggins *et al.*, Nature Nanotech. **1**, 137 (2006).
[10] G. Weber, J. W. Essex, and C. Neylon, Nature Phys. **5**, 769 (2009).
[11] M. Peyrard and A. R. Bishop, Phys. Rev. Lett. **62**, 2755 (1989).
[12] G. Maret, R. Oldenbourg, G. Winterling, K. Dransfeld, and A. Rupprecht, Colloid Polym. Sci. **257**, 1017 (1979).
[13] H. Grimm, H. Stiller, C. F. Majkrzak, A. Rupprecht, and U. Dahlborg, Phys. Rev. Lett. **59**, 1780 (1987).
[14] H. Grimm, P. M. Gehring, S. M. Shapiro, R. Kahn, and A. Rupprecht, Physica (Amsterdam) **213–214B**, 780 (1995).
[15] M. Krisch, A. Mermet, H. Grimm, V. T. Forsyth, and A. Rupprecht, Phys. Rev. E **73**, 61 909 (2006).
[16] Y. Liu *et al.*, J. Chem. Phys. **123**, 214909 (2005).
[17] A. Rupprecht, Biotechnol. Bioeng. **12**, 93 (1970).
[18] F. Merzel, F. Fontaine-Vive, M. R. Johnson, and G. J. Kearley, Phys. Rev. E **76**, 031917 (2007).
[19] A. Wildes, N. Theodorakopoulos, J. Valle-Orero, S. Cuesta-Lopez, J.-L. Garden, and M. Peyrard, Phys. Rev. Lett. **106**, 048101 (2011).
[20] R. Langridge, H. Wilson, C. Hooper, and M. W. L. Hamilton, J. Mol. Biol. **2**, 19 (1960).
[21] S. Arnott and D. W. L. Hukins, J. Mol. Biol. **81**, 93 (1973).
[22] W. Fuller, T. Forsyth, and A. Mahendrasingam, Phil. Trans. R. Soc. A **359**, 1237 (2004).
[23] H. Urabe, Y. Sugawara, M. Ataka, and A. Rupprecht, Biophys. J. **74**, 1533 (1998).
[24] See Supplemental Material at http://link.aps.org/supplemental/10.1103/PhysRevLett.107.088102 for additional descriptions and details.
[25] J. van Mameren, P. Gross, G. Farge, P. Hooijman, M. Modesti, M. Falkenberg, G. J. L. Wuite, and E. J. G. Peterman, Proc. Natl. Acad. Sci. U.S.A. **106**, 18 231 (2009).
[26] P. Gross, N. Laurens, L. B. Oddershede, U. Bockelmann, E. J. G. Peterman, and G. J. L. Wuite, Nature Phys. (2011).